Influence of the Ionic Strength on the Structure of Heat-Set Globular Protein Gels at pH 7. β-Lactoglobulin

Matthieu Pouzot, Dominique Durand, and Taco Nicolai*

Polymères, Colloïdes, Interfaces, UMR CNRS, Université du Maine, 72085 Le Mans Cedex 9, France

Received June 1, 2004; Revised Manuscript Received August 25, 2004

ABSTRACT: The effect of the NaCl concentration (C_s) on the structure factor and the turbidity of heat-set β-lactoglobulin gels and aggregates was investigated using light and X-ray scattering. Cross-correlation dynamic light scattering was applied to correct for multiple scattering in turbid systems. For $C_s \leq 50$ mM the gels are transparent and homogeneous on length scales above 20 nm, showing interaction peaks in small-angle X-ray scattering. For $C_s \geq 200$ mM the gels are opaque and heterogeneous on the micron length scale as shown by confocal scanning light microscopy. At intermediate salt concentrations the gels are characterized by a correlation length beyond which they are homogeneous, which decreases with increasing protein concentration and decreasing salt concentration. The fractal structure at smaller length scales is identical to that of the aggregates formed in dilute solution.

Introduction

Heat-induced denaturation of globular proteins leads to modification of their conformation, but they are not completely unfolded and keep their dense globular structure. This modification induces aggregation and, above a critical concentration, gelation.[1,2] The structure of the gels strongly depends on the pH and the ionic strength. In the presence of strong electrostatic repulsion, transparent gels are formed, while closer to the isoelectric point (pI) or at higher ionic strength the gels are turbid. Electron microscopy shows that gels and aggregates formed under strong electrostatic repulsion are fibrilar.[3−6] With decreasing interactions the aggregates are denser and more strongly branched. Confocal microscopy shows that at high ionic strength or close to pI the gels become heterogeneous on the micron scale.[7]

Using small-angle X-ray (SAXS) or neutron (SANS) scattering, it was found that the protein strands in transparent gels formed under strong electrostatic interactions are weakly ordered leading to the appearance of a so-called interaction peak.[6,8−10] The interaction peak disappears at higher ionic strength, and the scattering intensity becomes q-dependent at small q values that cannot be accessed by SAXS or SANS. To study the structure at larger length scales, light scattering is needed, but standard light scattering on turbid systems is perturbed by multiple scattering. Recently, however, it was shown that the structure of turbid protein gels can be studied using the 3-D cross-correlation dynamic light scattering technique.[11,12]

Using this technique, we have studied the structure of heat-set gels of β-lactoglobulin (β-lg) at pH 7 and 0.1 M NaCl over a range of concentrations.[12] We have shown that the structure can be described in terms of an ensemble of close-packed disordered "blobs" with a fractal internal structure that is identical to that of the aggregates that are formed initially. The blob size corresponds to the correlation length of concentration fluctuations, and the gels are homogeneous at length scales above the blob size. The correlation length decreases linearly with increasing concentration, but the structure at smaller length scales is independent of the protein concentration.

The objective of the present study is to investigate the influence of the electrostatic interactions on the structure of the gels and to relate it to the strongly varying turbidity. Electrostatic interactions can be varied by varying either the pH or the salt concentration. Here we have chosen to vary the salt concentration. In the present paper (part I) we present the results obtained for β-lg, and in the accompanying paper (part II) the results for ovalbumin are discussed.

β-lg is the main protein component in whey with molar mass 18.kg/mol and a radius of about 2 nm.[13,14] Heat-induced aggregation of β-lg at pH 7 is a two-step process.[15−18] During the first step well-defined primary aggregates are formed which contain, in the absence of added salt, about 100 proteins, i.e., with $M_w \approx 2 \times 10^6$g/mol, and their mass increases somewhat with increasing salt concentration.[18] However, the proteins do not aggregate at all below a very low critical concentration that decreases with increasing ionic strength.[18] At higher protein concentrations, the primary aggregates associate into fractal clusters with an average size that increases with increasing protein concentration and that diverges at C_g where the system gels. This process starts at increasingly higher protein concentrations if the salt concentration is lower, and C_g decreases with increasing ionic strength. Increasing the heating temperature accelerates the aggregation process but does not alter it.[19]

Materials and Methods

Materials. The β-lactoglobulin used in this study was a gift from Lactalis (Laval, France) and contained about equal fractions of the variants A and B for which the aggregation rate is equal in the mixture.[20] Solutions were extensively dialyzed against salt-free Milli-Q water at pH 7 with 200 ppm NaN_3 added to avoid bacterial growth. The salt concentration was set by addition of a concentrated NaCl solution. For light scattering measurements the samples were filtered through 0.45 μm pore size Anotope filters. The protein concentration was measured after filtration by UV absorption at 278 nm using extinction coefficient 0.96 L g^{-1} cm^{-1}. Solutions in airtight light scattering cells were heated for 24 h in a

* Corresponding author. E-mail: Taco.Nicolai@univ-lemans.fr.

10.1021/ma048919g CCC: $27.50
Published on Web 10/14/2004

thermostat bath at 80 °C, which is sufficient to complete the aggregation process, and subsequently rapidly cooled to 20 °C.

Light Scattering. Light scattering measurements were done at 20 °C using a commercial version of the 3D cross-correlation instrument described in ref 21 (LS Instruments, Fribourg, Switzerland). The light source was a diode laser with wavelength $\lambda = 685$ nm. Photon correlation was done with a digital correlator (ALV-5000E, ALV). The relative excess scattering intensity (I_r) was determined as the total intensity minus the solvent scattering divided by the scattering intensity of toluene at 20 °C. I_r was corrected for multiple scattering and the transmission as described in refs 11 and 12. The turbidity (τ) was determined at a wavelength of 685 nm using a spectrometer. The turbidity is calculated from the ratio of the light transmitted through the sample (I_s) and that transmitted though the solvent (I_0) using the following relation: $I_s/I_0 = \exp(-\tau l)$. The path length (l) was varied between 0.1 and 1 cm in order to have a significant signal at small τ and to minimize the effect of multiple scattering at large τ. In this way, turbidities between 0.1 and 10 cm^{-1} could be determined accurately.

SAXS. Synchrotron small-angle X-ray scattering measurements were performed at the Dutch-Flemish bending magnet BM26B "DUBBLE" beamline at the European Synchrotron Radiation Facility (ESRF) in Grenoble (France). The beamline optics provides an X-ray photon energy range of 6−35 keV. (In these experiments energies used were 12.2 and 8 keV, which correspond to the wavelengths of 0.1015 and 0.155 nm, respectively.) The range of scattering wave vectors covered was calibrated with the rat-tail collagen standard sample, and this range was $0.08 < q < 1.13$ nm^{-1}. The data collected on a 2D detector were reduced to the intensity profiles using radial averaging. The temperature was controlled by a thermostat bath and set at 20 °C. Absolute intensities were obtained by measuring native proteins with known molar mass.

Confocal Laser Scanning Microscope (CLSM) Observations. CLSM was used in the fluorescence mode. Observations were made in LPCM (INRA Nantes) with a Carl Zeiss LSM 410 Axiovert (Le Pecq, France), equipped with three lasers and four wavelengths available (364, 488, 543, and 633 nm). β-Lactoglobulin was labeled with a fluorochrome, rhodamine B isothiocyanate (RITC) (2.5 mg of RITC/g of β-Lg). The heat treatment (80 °C, 30 min) was applied using a thermostated stage (Linkam PE 60). Observation of β-Lg was made by excitation of RITC at 543 nm, the emission being recorded between 575 and 640 nm.

Results

β-lg solutions over a range of protein and salt concentrations were heated for 24 h at 80 °C. After this prolonged heat treatment the systems no longer evolve with heating time. If the NaCl concentration $C_s \leq 50$ mM, then the heated systems are transparent at all protein concentrations at least up to 120 g/L. At higher salt concentrations the turbidity increases with heating time to a constant value independent of heating temperature and duration. In Figure 1 we compare the concentration dependence of the turbidity (τ) of β-lg aggregates and gels formed after prolonged heating at $C_s = 100$, 150, and 200 mM. With increasing protein concentration the turbidity rises rapidly as C approaches C_g. (C_g is 7, 10, and 15 g/L for 200, 150, and 100 mM NaCl, respectively.) At 100 and 150 mM the turbidity stabilizes above C_g and even decreases at the highest concentrations, while at 200 mM the turbidity becomes too high and cannot be determined reliably above 10 g/L.

The structure factor ($S(q)$) was obtained using the cross-correlation technique by determining the scattering wave vector (q) dependence of I_r/HC as described in ref 12, where H is an optical constant. The results obtained at 100 mM were shown in ref 12, and Figure 2a shows the results for different concentrations at 150 mM. Extrapolation of I_r/HC to $q = 0$ yields an apparent molar mass, M_a, which is inversely proportional to the osmotic compressibility. In ref 12 we showed that at 100 mM the data obtained at different concentrations can be superimposed by plotting the structure factor $S(q) = I_r/(HCM_a)$ as a function of qR_a, where R_a is the apparent radius of gyration. Good superposition is also obtained at 150 mM (see Figure 2b). Similar results are obtained at 200 mM, but because of the high turbidity,

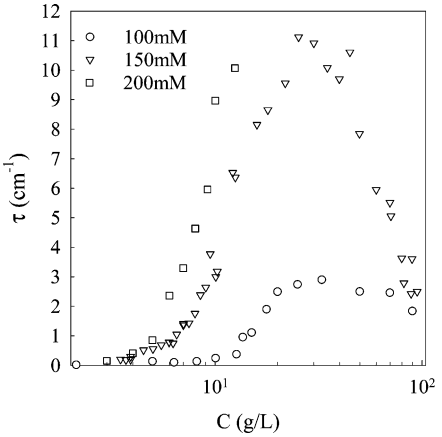

Figure 1. Concentration dependence of the turbidity at 685 nm for β-Lg solutions at pH 7 and various NaCl concentrations indicated in the figure, after prolonged heating at 80 °C.

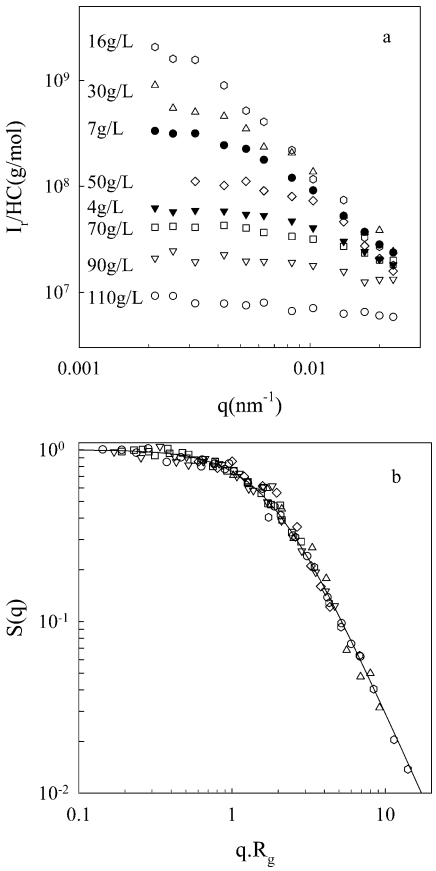

Figure 2. (a) Scattering wave vector dependence of I_r/HC for β-lactoglobulin solutions at different concentrations indicated in the figure after prolonged heating at 80 °C (pH 7 and 150 mM NaCl). Filled symbols represent solutions, and open symbols represent gels. (b) Structure factor of β-lactoglobulin solutions obtained by normalization of the data shown in (a). The solid line represents $S(q) = (1 + q^2R_a^2/3)^{-1}$.

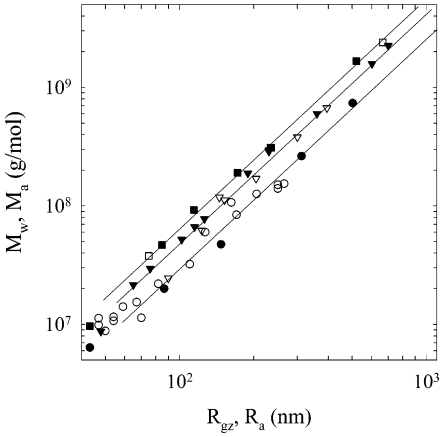

Figure 3. Comparison of the dependence of M_a on R_a (open symbols) with that of M_w on R_{gz} (filled symbols) at different NaCl concentrations. The symbols are as in Figure 1. The solid lines have slope 2.

the structure factor could be determined only over a limited range of low concentrations. At all three ionic strengths, the structure factor is well described by the following simple equation:

$$S(q) = (1 + q^2R_a^2/3)^{-1} \quad (1)$$

For self-similar, fractal objects $S(q) \propto q^{-d_f}$ over the q range where the fractal structure is probed.[22,23] The implication of eq 1 is that the structures of the systems are homogeneous at length scales larger than R_a and self-similar at length scales below R_a characterized by a fractal dimension $d_f = 2$. The heated systems may be visualized as a randomly distributed collection of blobs with z-average radius of gyration R_a and weight-average molar mass M_a.

An independent verification of the fractal structure can be obtained by plotting M_a as a function of R_a. Figure 3 shows that $M_a = aR_a^2$, which confirms that the structure is indeed fractal with $d_f = 2$ for large values of M_a. The prefactor a increases with increasing ionic strength: $a = 2.9 \times 10^3$, 4.4×10^3, and 6.2×10^3 at 100, 150, and 200 mM, respectively (with M_a and R_a in g/mol and nm, respectively). The relationship between M_a and R_a is compared in Figure 3 to that between the weight-average molar mass, M_w, and the z-average radius of gyration, R_{gz}, of the aggregates formed at $C < C_g$, that were obtained from light scattering measurements after strongly diluting the aggregates. The dependence of M_w on R_{gz} shown in Figure 3 at 100 and 200 mM NaCl was taken from ref 18, and it was determined in the same way at 150 mM. Within the experimental error, the relationship between M_a and R_a is the same as that between M_w on R_{gz}, which implies that the blobs have the same structure as the aggregates. The increase of the prefactor a with increasing ionic strength implies that the local structure of the aggregates is denser at higher salt concentrations (see ref 6).

The concentration dependence of the R_a is shown in Figure 4. R_a increases rapidly with increasing concentration for C close to C_g, but at higher concentrations it decreases again at 100 and 150 mM, while at 200 mM the systems could not be studied at higher concentrations. The open symbols in Figure 4 show the values of R_a deduced from the turbidity data, which will be discussed below. For $C_s \leq 50$ mM, the structure factor

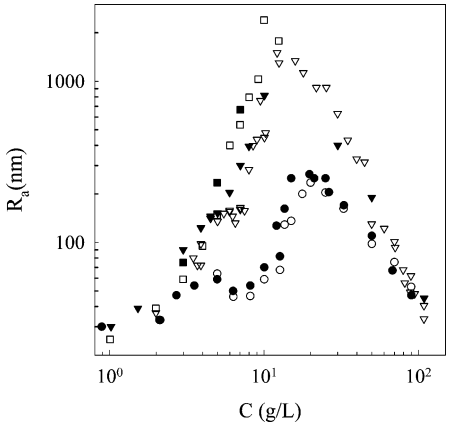

Figure 4. Concentration dependence of R_a at different NaCl concentrations. The filled symbols represent values determined directly using cross-correlation dynamic light scattering, while the open symbols represent values deduced from the turbidity. The symbols are as in Figure 1.

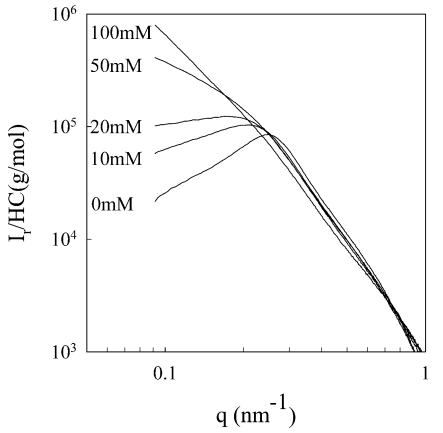

Figure 5. Scattering wave vector dependence of I_r/HC obtained from SAXS for β-lg gels at 100 g/L and different NaCl concentrations indicated in the figure obtained after prolonged heating at 80 °C.

is unity over the whole q range covered by the light scattering technique because strong electrostatic interactions render the system homogeneous. SAXS is needed in order to observe the structural organization at smaller length scales. In Figure 5 we show SAXS results of gels formed at different ionic strengths for $C = 100$ g/L. With decreasing salt concentration the scattering at low q values, i.e., in the light scattering range, is decreased leading to a so-called interaction peak for $C_s \leq 20$ mM. The interaction peak indicates a weak ordering of the aggregated proteins, which decreases if the protein concentration is lower.[6]

For $C_s \leq 50$ mM the structure factor is not described by eq 1, and we did not attempt to determine a correlation length, which is less than 20 nm. On the other hand, M_a is easily measured using light scattering, and Figure 6 shows the concentration dependence of M_a at 0, 50, and 100 mM NaCl. We note that in all cases 3 mM NaN_3 is added as a bacteriostatic agent. At 100 mM, M_a increases strongly at C_g and passes through a maximum consistent with the concentration dependence of R_a, but at 0 and 50 mM M_a decreases continuously with increasing concentration.

For comparison, we also show in Figure 6 the weight-average molar mass of the aggregates (M_w) formed at $C < C_g$. At low protein concentrations interactions are weak, and $M_a \approx M_w$ except at concentrations close to

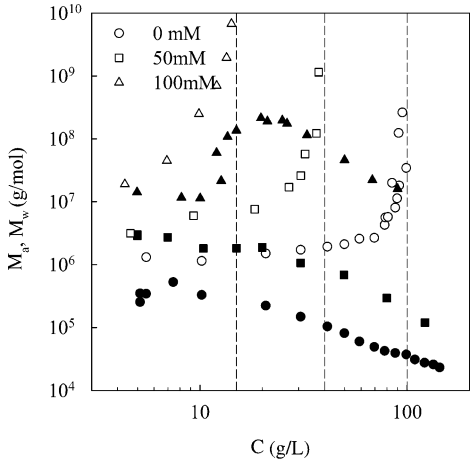

Figure 6. Comparison of the concentration dependence of M_w (open symbols) and M_a (filled symbols) at different NaCl concentrations indicated in the figure. The dashed lines indicate C_g.

the critical association concentration where M_a is influenced by the presence of unaggregated proteins. The critical concentration for the formation of primary aggregates is 3, 0.5, and 0.2 g/L for 0, 50, and 100 mM, respectively,[18] and the effect is only visible in Figure 6 for the results obtained in the absence of NaCl.

With increasing protein concentration repulsive interactions between the aggregates become increasingly important so that M_a is less than M_w. For $C_s \leq 50$ mM, the effect of electrostatic repulsion dominates over that of the growth of the aggregates and M_a decreases continuously, starting from the molar mass of the primary aggregates. For $C > 50$ mM, M_a increases first as M_w rises rapidly close to C_g, but at higher concentrations again repulsive interactions dominate and M_a (R_a) decreases.

Discussion

The visual aspect of β-lg gels at pH 7 varies strongly over a small range of NaCl concentrations from transparent at 50 mM to practically opaque at 200 mM. Qualitatively, the strong increase of the turbidity can be understood in terms of the increasing heterogeneity (correlation length) of the gels. For a quantitative explanation we can use the relation between the turbidity and the structure factor:[12]

$$\tau = H'CM_a\int_0^{2\pi}\int_0^{\pi}S(q)(1+\cos^2\theta)\sin\theta\,\mathrm{d}\theta\,\mathrm{d}\varphi \quad (2)$$

where H' is another optical constant. Despite the strongly varying turbidity, the structure factor of the heated β-lg solutions is not changed between 100 and 200 mM and is independent of the protein concentration. The simple form of $S(q)$ allows one to relate the turbidity to the structural parameters M_a and R_a:

$$\tau = H'CM_a 2\pi\left[\frac{-4}{a^2}(a+2)+\frac{8a+4a^2+8}{a^3}\ln(1+a)\right] \quad (3)$$

with

$$a = \left(\frac{4\pi n}{\lambda}\frac{R_a}{\sqrt{3}}\right)^2$$

If in addition we use the power law relation between M_a and R_a shown in Figure 3, it is possible to deduce R_a from the turbidity. The results are included in Figure 4 and are consistent with the directly measured values of R_a, although for small values of R_a the power law relationship with M_a is only approximate. Using the quantitative relationship between τ and R_a is very advantageous because the turbidity can be measured much more simply and rapidly than R_a. Once $S(q)$ and the relationship between M_a and R_a have been established for a relatively small number of samples, the concentration dependence of R_a can be studied in detail using the turbidity. In the present case, the relationship between τ and R_a is simple and can be expressed analytically, but in general, eq 3 will have to be resolved numerically.

The balance between the increase of M_w and R_{gz}, which dominates at low concentrations, and the increase of repulsive excluded-volume and electrostatic interactions, which dominates at high concentrations, determines the concentration dependence of M_a and R_a. In the presence of 100 mM NaCl the concentration dependence can be roughly understood considering only excluded-volume interactions, as was discussed in detail in ref 12. At low concentrations the aggregates are still relatively dilute and $R_a \approx R_{gz}$. As the concentration increases, the cumulated volume fraction (ϕ) occupied by the aggregates increases:

$$\phi = \sum C_i \frac{4\pi {R_{gi}}^3 N_a}{3M_i} \quad (4)$$

where C_i is the concentration of aggregates with radius of gyration R_{gi} and molar mass M_i, and N_a is Avogadro's number. Increasing excluded-volume interaction causes the measured apparent molar mass and radius of gyration to be less than R_{gz} and M_w. On small length scales the structure of the system is the same as that of dilute aggregates, but on larger length scales excluded-volume interactions are screened by the overlap or interpenetration of other aggregates. The interpenetration of the aggregates renders the system homogeneous at length scales larger than R_a when $\phi > 1$. In analogy with semidilute polymer solutions[24] we may visualize the system as a collection of disordered blobs with size R_a and molar mass M_a that fill up the whole space. The cumulated volume fraction of the aggregates diverges at C_g while that of the blobs becomes a constant of order unity.

In Figure 7 we compare the concentration dependence of the cumulated volume fraction of the aggregates (ϕ_a) and the blobs (ϕ_b) at 100 and 150 mM NaCl. ϕ was calculated using eq 4 and assuming that the aggregates and the blobs are monodisperse with R_g and M equal to R_{gz} and M_w or M_a and R_a, respectively. In all cases ϕ_a diverges at the gel point because $\phi_a \propto {M_w}^{0.5}$, where we used $C4\pi {R_{gz}}^3 N_a/3M_w$ and $M_w \propto {R_{gz}}^2$.

At 100 mM we find that indeed ϕ_b becomes a constant above C_g so that the image of heated proteins as a collection of monodisperse fractal blobs appears reasonable at this salt concentration. As discussed in ref 12, it follows from eq 4 that if ϕ_b is constant and $M_a \propto {R_a}^{d_f}$, then $R_a \propto C^{(d_f-3)}$.

At 150 mM ϕ_b becomes much larger than unity close to C_g and decreases with increasing concentration above C_g. We speculate that this is caused by heterogeneity of the system, which decreases with increasing protein

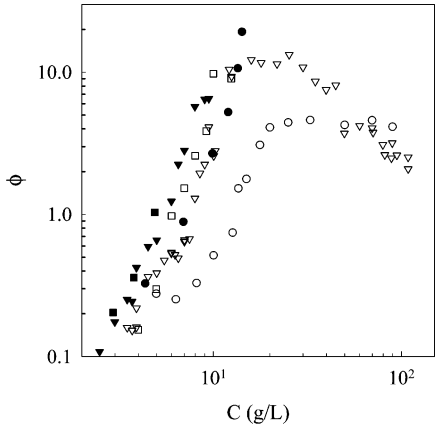

Figure 7. Comparison of the cumulated volume fraction of the aggregates (filled symbols) and the blobs (open symbols) at different NaCl concentrations. The symbols are as in Figure 1.

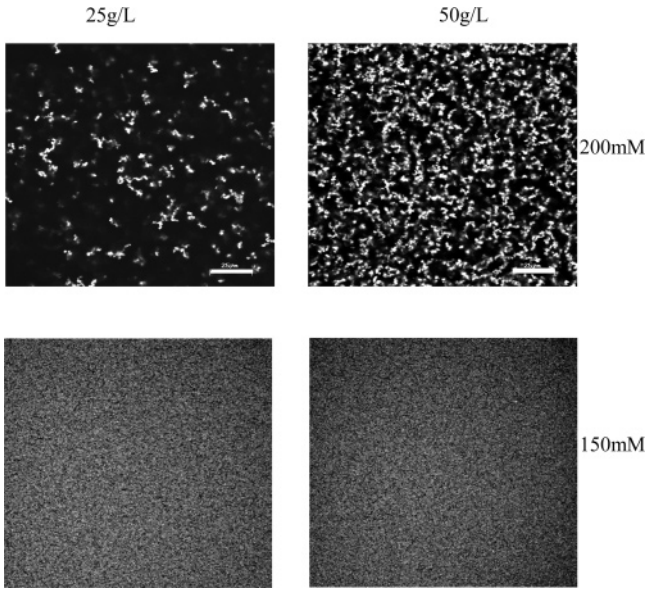

Figure 8. Confocal microscopy images of heat-set gels *β*-lg gels formed after heating at 150 and 200 mM NaCl. The bar represents 25 μm.

concentration. In other words, we may visualize this system as a collection of polydisperse blobs. For a polydisperse system ϕ_b is overestimated if calculated using $\phi_b = (C4\pi R_a{}^3 N_a)/(3M_a)$ because R_a represents a *z*-average and M_a a weight-average. The overestimation becomes less important with increasing protein concentration because the system becomes more homogeneous.

At 200 mM the heterogeneity, and as a consequence R_a, M_w, and τ, become very large, and light scattering can no longer be used to characterize the structure. In this case, the structure can be visualized using confocal scanning light microscopy. Figure 8 shows a comparison of confocal microscopy images of gels formed after heating at 150 and 200 mM NaCl. Below 150 mM NaCl the structure cannot be resolved with the confocal microscope because the gels are homogeneous on length scales larger than 500 nm. At 150 mM some structure can be seen, albeit close to the limit of the resolution, but at 200 mM the structure can be clearly observed, confirming that the gels are heterogeneous on large length scales not accessible to light scattering measurement.

Conclusion

β-Lactoglobulin gels at pH 7 formed after prolonged heating are homogeneous above a characteristic length scale that decreases with increasing protein concentration. In the absence of added salt, strong electrostatic interactions lead to weakly ordered systems with a structure factor that is characterized by an interaction peak at large *q* values accessible only in SAXS or SANS experiments.

With increasing salt concentration the interaction peak progressively disappears, and the structure factor above 50 mM NaCl can be described by eq 1. The structure of the gels at higher salt concentrations can be visualized as a collection of blobs with a fractal local structure that is identical to that of the aggregates formed in dilute solutions. The average blob size decreases with increasing concentration and decreasing salt concentration. Above 150 mM NaCl the heterogeneity of the gels is on the micron scale and cannot be characterized using light scattering, but it can be visualized using confocal microscopy.

The variation of the turbidity with the protein and the salt concentration can be quantitatively related to the molar mass and radius of the blobs.

Acknowledgment. We thank Laurence Donato for performing the confocal scanning light microscopy experiments at the INRA (Nantes, France). Igor Dolbnya and Wim Bras are thanked for their technical assistance at the DUBBLE (Grenoble, France). We thank Unilever (Colworth, U.K.) for financial support.

References and Notes

(1) Clark, A. H. In *Functional Properties of Food Macromolecules*, 2nd ed.; Hill, S. E., Ledward, D. A., Mitchell, J. R., Eds.; Aspen Publishers: Gaithersburg, MD, 1998; p 77.
(2) Gosal, W.; Murphy, S. B. *Curr. Opin. Colloid Interface Sci.* **2000**, *5*, 188.
(3) Aymard, P.; Nicolai, T.; Durand, D.; Clark, A. *Macromolecules* **1999**, *32*, 2542.
(4) Gosal, W. S.; Clark, A. H.; Pudney, P. D. A.; Ross-Murphy, S. B. *Langmuir* **2002**, *18*, 7174.
(5) Veerman, C.; Sagis, L. M. C.; Heck, J.; van der Linden, E. *Int. J. Biol. Macromol.* **2003**, *31*, 139.
(6) Weijers, M.; Visschers, R. W.; Nicolai, T.; Pouzot, M. *Food Hydrocolloids*, in press.
(7) Verheul, M.; Roefs, S. P. F. M.; De Kruif, K. G. *J. Agric. Food Chem.* **1998**, *46*, 896.
(8) Renard, D.; Axelos, A.; Lefebvre, J. In *Food Macromolecules and Colloids*; Dickenson, E., Lorient, D., Eds.; Royal Society of Chemistry: Cambridge, 1995; p 390.
(9) Clark, A. H.; Tuffnell, C. D. *Int. J. Peptide Res.* **1980**, *16*, 339.
(10) Weijers, M.; Visschers, R. W., unpublished results.
(11) Nicolai, T.; Urban, C.; Schurtenberger, P. *J. Colloid Interface Sci.* **2001**, *240*, 419.
(12) Pouzot, M.; Nicolai, T.; Durand, D.; Benyahia, L. *Macromolecules* **2004**, *37*, 614.
(13) Papiz, M. Z.; Sawyer, L.; Eliopoulos, E. E.; North, A. C. T.; Findlay, J. B. C.; Sivaprasadarao, R.; Jones, T. A.; Newcomer, M. E.; Kraulis, P. J. *Nature (London)* **1986**, *324*, 383.
(14) Pessen, H.; Kumosinski, T. F.; Farrell, H. M. J. *J. Ind. Microbiol.* **1988**, *3*, 89.
(15) Aymard, P.; Gimel, J. C.; Nicolai, T.; Durand, D. *J. Chim. Phys.* **1996**, *93*, 987.
(16) Le Bon, C.; Nicolai, T.; Durand, D. *Int. J. Food Sci. Technol.* **1999**, *34*, 451.
(17) Durand, D.; Gimel, J. C.; Nicolai, T. *Physica A* **2002**, *304*, 253.
(18) Baussay, K.; Le Bon, C.; Durand, D.; Nicolai, T.; Busnel, J. P. *Int. J. Biol. Macromol.* **2004**, *34*, 21.
(19) Le Bon, C.; Nicolai, T.; Durand, D. *Macromolecules* **1999**, *32*, 6120.

(20) Le Bon, C.; Durand, D.; Nicolai, T. *Int. Dairy J.* **2002**, *12*, 671.
(21) Urban, C.; Schurtenberger, P. *J. Colloid Interface Sci.* **1998**, *207*, 150.
(22) Higgins, J. S.; Benoit, H. C. *Polymers and Neutron Scattering*; Clarendon Press: Oxford, 1994.
(23) Brown, W., Ed. *Light Scattering. Principles and Developments*; Clarendon Press: Oxford, 1996.
(24) de Gennes, P. G. *Scaling Concepts in Polymer Physics*; Cornell University Press: Ithaca, NY, 1979.

MA048919G